Title

Dihydromyricetin ameliorates social isolation-induced anxiety by modulating mitochondrial function, antioxidant enzymes, and BDNF

Authors

Al Omran, Alzahra J
Watanabe, Saki
Hong, Ethan C
et al.

Publication Date

2022-11-01

DOI

10.1016/j.ynstr.2022.100499

Neurobiology of Stress 21 (2022) 100499

Contents lists available at ScienceDirect

Neurobiology of Stress

journal homepage: www.elsevier.com/locate/ynstr

Dihydromyricetin ameliorates social isolation-induced anxiety by modulating mitochondrial function, antioxidant enzymes, and BDNF

Alzahra J. Al Omran [a,1], Saki Watanabe [a,1], Ethan C. Hong [a], Samantha G. Skinner [a], Mindy Zhang [a], Jifeng Zhang [a], Xuesi M. Shao [b], Jing Liang [a,*]

[a] Titus Family Department of Clinical Pharmacy, University of Southern California School of Pharmacy, Los Angeles, CA, 90033, USA
[b] Neurobiology, David Geffen School of Medicine at UCLA, Los Angeles, CA, 90095, USA

ARTICLE INFO

Keywords:
Stress
Anxiety
Dihydromyricetin (DHM)
Mitochondria
Antioxidative enzymes
Oxidative stress
Autophagy
BDNF
BDNF-TrkB
Social isolation
Repeated social isolation

ABSTRACT

Stress has been implicated in the etiology of neurological and psychological illnesses. Chronic social isolation (SI) is a psychological stressor that provokes neurobehavioral changes associated with psychiatric disorders, including anxiety disorders. Mitochondria dysfunction and oxidative stress are hallmarks of anxiety pathogenesis. Here we demonstrate the effects of SI-induced stress on mitochondrial function, antioxidative enzymes, autophagy, and brain derivative neurotrophic factor (BDNF). SI induced a reduction in electron transport chain subunits C–I, C-II, and C-VI and an increase in hydrogen peroxide. Treatment with dihydromyricetin (DHM), extracted from *Ampelopsis grossedentata*, counteracted these changes. A dramatic increase in several primary mitochondrial antioxidative enzymes such as superoxide dismutase 2 (SOD2), heme oxygenase-1 (HO-1), peroxiredoxin-3 (PRDX3), and glutathione peroxidase 4 (GPX4) was observed after SI and a repeated episode of SI. Both SI and repeated SI induced a reduction in sequestosome 1 (SQSTM1/p62). However, only repeated SI modulated autophagy primary protein beclin-1 (Bcl-1). In addition, SI and repeated SI modulated the BDNF-TrkB signaling pathway and the phosphorylation of the downstream extracellular signal-regulated MAP kinase1/2 (p-Erk p42 and p-Erk p44) cascade. DHM treatment ameliorated these changes. Collectively, we demonstrated that DHM treatment counteracted the effects of SI and repeated SI on antioxidative enzymes, autophagy, and the BDNF-TrkB signaling pathway. These findings highlight the molecular mechanisms that partially explain the anxiolytic effects of DHM.

1. Introduction

Anxiety disorders are the most prevalent mental illness in the U.S. Current estimates suggest that more than 40 million (18%) adults are suffering from anxiety disorders, which imposes a great economic burden on public health and accounts for more than $42 billion in costs for medical evaluation and treatment (Facts and Statistics, 2016). Anxiety disorders are often comorbid with depression, posttraumatic stress disorder (PSTD), substance use disorders, and subsequent cognitive impairment (Kessler et al., 2010; Becker et al., 2018). Various psychological stressors contribute to the pathophysiology of anxiety disorders, which include environmental, socioeconomic, and genetic factors (Nugent et al., 2011; Hettema et al., 2005). Furthermore, modern society's social and demographic changes have increased loneliness and social isolation (Klinenberg, 2016; Beutel et al., 2017). This phenomenon is further exacerbated by the coronavirus disease 2019 (COVID-19) pandemic, which has led to global social isolation that negatively impacts the public's mental and psychological wellbeing and creates heightened anxiety disorders (Twenge and Joiner, 2020; Loades et al., 2020). As a result of the pandemic, there was an estimated 26% elevation in anxiety disorders rate globally from 2020 to 2021 (Collaborators, 2021). Despite the high prevalence of anxiety, effective and safe therapies are still considered an unmet medical need. Unfortunately, not all patients respond well to the currently available treatments, and some have treatment resistance, leaving more than 40% of the patient population lacking effective medications (Roy-Byrne, 2015).

The inhibitory neurotransmitter ɣ-aminobutyric acid (GABA) has long been recognized as the primary modulator in anxiety disorders (Nuss, 2015). An increasing number of studies have implied the association of neuroinflammation, mitochondrial dysfunction, and oxidative

* Corresponding author.
E-mail address: jliang1@usc.edu (J. Liang).
[1] These authors contributed equally to this work.

https://doi.org/10.1016/j.ynstr.2022.100499
Received 27 May 2022; Received in revised form 24 October 2022; Accepted 26 October 2022
Available online 30 October 2022

stress pathways in the pathogenesis of anxiety (Zlatković et al., 2014a, 2014b; Shao et al., 2015). Previous work from our group showed dysregulation in the hypothalamic-pituitary-adrenal (HPA) axis, manifesting as an increase in serum corticosteroid levels in the social isolation (SI)-induced anxiety mouse model, which is considered an indicator of stress (Al Omran et al., 2022). Furthermore, SI mice showed signs of neuroinflammation through activation of the NF-kB signaling pathway that triggered microglia morphological changes (Al Omran et al., 2022). Additionally, we demonstrated that SI induces an alteration in mitochondrial energy metabolism represented by a reduction in ATP level (Silva et al., 2020). Neuroinflammation negatively impacts mitochondrial viability and contributes to neuronal excitotoxicity, oxidative stress damage, energy depletion, neurogenesis impairment, and eventually neuronal death (Li et al., 2017; Banagozar Mohammadi et al., 2019). Therefore, distressed mitochondria also provoke further neuroinflammation, creating a constant pathological cycle between neuroinflammation, mitochondrial impairment, oxidative stress, and neurotoxicity. In the present study, we further investigated the effect of psychological stress on mitochondrial function, the antioxidative defense system, autophagy, and the brain-derived neurotrophic factor (BDNF) pathway utilizing a SI mouse model. Moreover, we investigated the impact of repeated SI stress on mitochondrial function, oxidative stress, autophagy, and the BDNF pathway. These observations were examined in the prefrontal cortex (PFC) due to its essential role in regulating fear and anxiety emotions by integrating inputs from the amygdala and the hippocampus (Burgos-Robles et al., 2009).

Previously, we have shown that dihydromyricetin (DHM) [(2R,3R)-3,5,7-trihydroxy-2-(3,4,5-trihydroxyphenyl)-2,3-dihydrochromen-4-one], a primary plant bioactive flavonoid extracted from *Ampelopsis grossedentata*, is a positive modulator of the $GABA_A$ receptor ($GABA_AR$) (Silva et al., 2020; Liang et al., 2014). It antagonizes the detrimental effects of acute and chronic ethanol consumption on $GABA_ARs$ in animal models (Liang et al., 2014; Shen et al., 2012). Furthermore, we previously demonstrated that DHM exerts anxiolytic effects in SI mouse model by improving GABAergic neurotransmission and $GABA_AR$ function (Silva et al., 2020). Therefore, DHM's effect on GABA provides one possible mechanism for its ability to improve anxiety-like behaviors in SI mice. Notably, GABAergic transmission impairment is a primary factor in neurotoxicity that provokes a chain of events, including mitochondrial dysfunction, changes in antioxidant enzyme activity, oxidative stress, and neuroplasticity dysfunction. This triggers several cellular pathways leading to behavioral deficits (Chanana and Kumar, 2016; Zhu et al., 2019). Therefore, studying the effects of DHM on mitochondria, antioxidative enzyme activity, and BDNF is essential in elucidating the mechanism of DHM's anxiolytic action. This study will help gain insight into the cellular and molecular aspects of anxiety disorders, which is a crucial step in developing novel and effective therapeutics. In addition, this study will expand our understanding of DHM's anxiolytic mechanisms and set the stage for DHM to be a therapy for anxiety disorders.

2. Methods

2.1. Animals and treatment

2.1.1. Experimental design

Eight-week-old male C57BL/6 mice (Charles River Laboratories) were housed in the vivarium under controlled temperature, humidity, and 12 h light/dark cycles with free access to food and water. All animal experiments were performed according to the protocols approved by the University of Southern California (USC) Institutional Animal Care and Use Committee. Mice were randomly assigned to either a group-housed group (2–4 mice/cage) or an isolated group. SI mice were singly housed in opaque-walled cages with reduced bedding, no environmental enhancers (toys/objects), and minimal human handling with the exception of weekly cage changes. The treatment groups were organized as described below:

A. Social isolation (SI) for 4 weeks phase: Animals were either grouped or singly housed for 2 weeks, followed by 2 weeks of treatment (Fig. 1A).

1. Group-housed, 2–4 mice/cage, and administered vehicle (sucrose) (G + V), n = 11
2. Group-housed, 2–4 mice/cage, and administered DHM 2 mg/kg (G + D), n = 11
3. Social-isolated, single-housed, and administered vehicle (sucrose) (SI + V), n = 14
4. Social-isolated, single-housed, and administered DHM 2 mg/kg (SI + D), n = 14

After the 4-week-SI phase, four mice from each group were randomly selected to test the effect of anxiety withdrawal, followed by a second isolation period. Mice designated for the isolation group were group-housed for 4 weeks, followed by another 4 weeks of isolation. The group-housed mice were grouped in the same cage for the rest of the experiment period as shown in (Fig. 1B).

B. Social isolation withdrawal period followed by repeated social isolation phase:

1. Group-housed, 2–4 mice/cage and administered vehicle (sucrose) (G + V), n = 4
2. Group-housed, 2–4 mice/cage and administered DHM 2 mg/kg (G + D), n = 4
3. Isolated, single-housed, and administered vehicle (sucrose) (R–SI + V), n = 4
4. Isolated, single-housed, and administered DHM 2 mg/kg (R–SI + D), n = 4

This model has been used in our previous studies and consistently exhibits anxious behaviors. A detailed protocol of the model can be found on Watanabe et al., 2022 (DOI:10.3791/64567). Anxiety behaviors based on open field test and elevated plus maze of these mice can be found on Al Omran et al., 2022. The same mice cohort/samples were used in this study.

2.1.2. Drug preparations

DHM (HPLC purified ≥98%, Master Herbs Inc., Pomona, CA) was given orally as an agar cube once per day (2 mg/kg) for 2 weeks (Silva et al., 2020). DHM and vehicle agar cubes were prepared using 3% agar with water and then heated to ~90 °C to dissolve the agar. Subsequently, DHM + 5% sucrose (for DHM group) or 5% sucrose only (for vehicle group) was added and mixed until cooled and solidified. Then, the agar was cut into cubes of 0.5 × 0.5 × 0.5 cm each.

2.1.3. Drug administration

During the dark cycle, the mice were given DHM or vehicle by placing the agar cube in a 50 × 50 × 8 mm weighing dish and placing it in the cage after removing all food. To give the treatment for group-housed, mice were separated, fed DHM or vehicle, and then returned to the group housing cage. All animals were observed to ensure complete consumption of agar, which took 30–90 min.

2.1.4. Hydrogen peroxide assay

Mice were dissected after 4 weeks of social isolation and 12 weeks of repeated social isolation. The amount of H_2O_2 in the prefrontal cortex (PFC) tissue was measured using a hydrogen peroxide assay kit (ab102500, Abcam, Cambridge, MA, USA) according to the manufacturer's instructions. The PFC tissues were collected and lysed in ice-cold assay buffer provided by the kit. The supernatants were collected, deproteinized, and incubated in a working solution containing OxiRed probe and horseradish peroxidase (HRP). The intensity of the color developed was measured at 570 nm using a Synergy H1 Hybrid Multi-Mode Reader (BioTek).

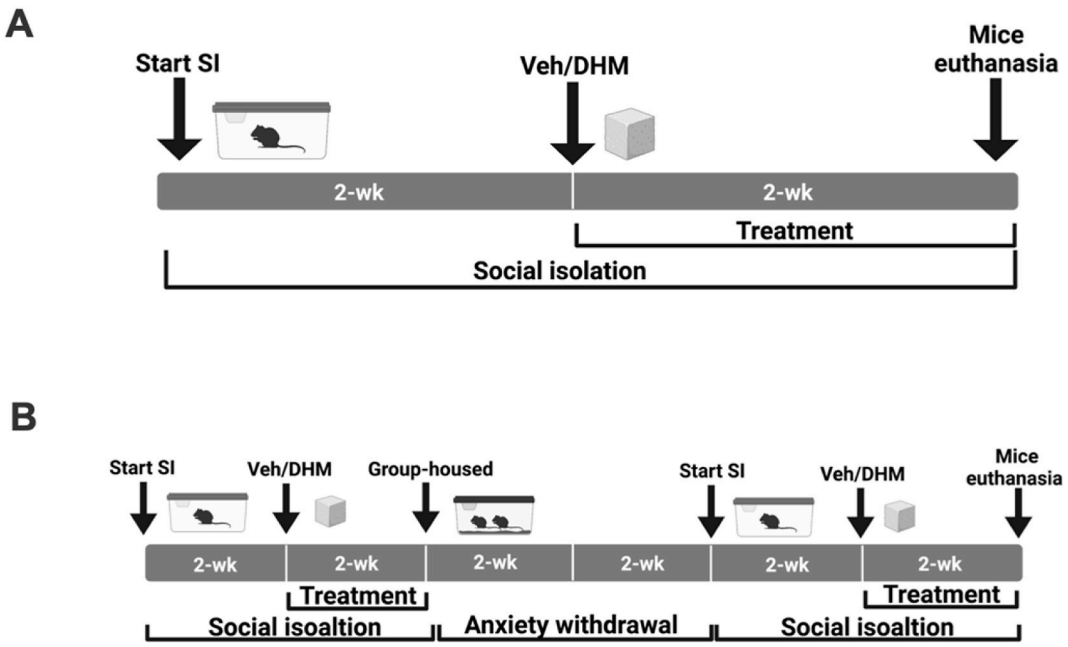

Fig. 1. Study design and timeline of the experiments. (A) Mice were single housed for 2 weeks followed by 2 weeks of DHM 2 mg/kg treatment. **(B)** Mice were single housed for 2 weeks followed by 2 weeks of DHM 2 mg/kg treatment. The same group of mice was group-housed (SI-withdrawal) for 4 weeks, then another 2 weeks repeated SI, then 2 weeks of DHM 2 mg/kg treatment. The group-housed mice (G + V and G + D) remained group-housed for the entire length of the study.

2.2. Mitochondria complex assays

The colorimetric complex enzyme activity assay kits (ab109721, ab109908, and ab109911, Abcam, Cambridge, MA, USA) were used to detect the activity of complexes I, II, and IV in isolated mitochondria from the PFC. Mitochondria were isolated according to the manufacturer's guidelines (ab110168, Abcam) and 25 μg of mitochondria were loaded per well. After sample preparation and plate incubation, based on the manufacturer's guidelines, samples were read at 450 nm in 1-min intervals for 30 min for complex I, 600 nm in 20-s intervals for 60 min for complex II, and 550 nm in 1-min intervals for 2 h for complex IV. All readings were performed between 25 and 30 °C using Synergy H1 Hybrid Multi-Mode Reader (BioTek). The linear rate of increase in absorbance at OD 450 nm, 600 nm, or 550 nm were calculated over time and plotted on a bar graph using the equation provided on the guidelines:

$$\text{Rate mOD/min} = (\text{Absorbance1} - \text{Absorbance2})/(\text{Time1} - \text{Time2})$$

2.2.1. Western blot analysis

Equal protein concentrations of PFC homogenates were separated on 10% sodium dodecyl sulfate-polyacrylamide gel electrophoresis and then transferred to PVDF membranes (Bio-Rad Laboratories, Hercules, CA). Membranes were blocked in 5% skim milk in 1X Tris-buffered saline with Tween 20 (TBST) for 1 h at room temperature. Membranes were then incubated overnight (4 °C) with either mouse anti-mouse OxPhos antibody cocktail (Thermo Fisher 45–8099, 1:200), mouse anti-mouse β-actin (Cell Signaling 4970, 1:1000), rabbit anti-mouse (mAb) SOD-2 (Cell Signaling 13141, 1:1000), rabbit mAb HO-1 (Cell Signaling 86806, 1:1000), rabbit mAb PRDX-3 (Abcam ab73349, 1:1000), rabbit mAb GPX-4 (Cell Signaling 52455, 1:1000), Bcl-1 rabbit mAb Cell Signaling 42406, 1:1000), p62 rabbit mAb Cell Signaling 23214, 1:1000), BDNF (Cell Signaling 47808, 1:1000), p-TrkB (Abcam ab229908, 1:1000), p44/42 MAPK (Erk1/2) (Cell Signaling L34F12, 1:1000), Phospho-p44/42 MAPK (Erk1/2) (Cell Signaling D13.14.4E, 1:1000). After washing three times with 1X TBST, the membranes were incubated in a secondary antibody goat anti-rabbit IgG or goat anti-mouse (Bio-Rad 1706515 and 1706516) in 1X TBST for 1 h. Blots were subsequently developed with an enhanced chemiluminescence (ECL) system (Bio-Rad 1705061) and visualized using a Chemi-Doc (Bio-Rad) imaging device.

2.2.2. SOD activity

The colorimetric superoxide dismutase activity assay kit (ab65354, Abcam, Cambridge, MA, USA) was used to detect the activity of SOD in PFC homogenates. According to the manufacturer's instructions, each sample requires three blanks to calculate the inhibition rate in a 96 well plate. Blank-1 contained dH_2O + enzyme working solution, blank-2 with sample alone, and blank-3 with dH_2O alone in addition to the fourth well of the sample + enzyme working solution. The intensity of the developed color was measured at $\lambda = 450$ nm using Synergy H1 Hybrid Multi-Mode Reader (BioTek). The OD values were used to calculate the SOD activity expressed as the inhibition rate following the equation listed in the instruction.

$$\text{SOD Activity (inhibition rate \%)} = [(\text{blank1} - \text{blank3}) - (\text{sample} - \text{blank2}) \times 100]/ (\text{blank1} - \text{blank} \quad 3)$$

2.3. ELISA analysis

PFC tissue lysates were homogenized in RIPA lysis buffer (89900, Thermo Scientific, Milford, MA). The homogenates were then used to quantify BDNF protein concentration using an ELISA kit and following the manufacturer's protocol (DBNT00, R&D Systems, Minneapolis, MN, USA). The intensity of the color developed was measured using a Synergy H1 Hybrid Multi-Mode Reader (BioTek).

2.4. Statistical analysis

All assays were performed at least three times. The data were presented as the mean ± standard error of the mean using GraphPad Prism 9 (GraphPad Software, Inc., La Jolla, CA). We performed two-way analysis of variance (ANOVA, two factors: housing and treatment with interaction term) and report the F value of the interaction and its p

value. We then perform Holm-Sidak multiple comparison test (SigmaStat, version 3.5), and the significance level was set at $p \leq 0.05$.

3. Results

3.1. The effect of social isolation, repeated social isolation, and DHM treatment on reactive oxygen species (ROS) formation and mitochondrial complex I, II, and IV protein expression

To assess the levels of reactive oxygen species (ROS) production after SI, hydrogen peroxide (H_2O_2) activity was measured. H_2O_2 is a common reactive oxygen metabolic byproduct and a potent inducer of oxidative stress (Hou et al., 2015). The level of H_2O_2 was substantially higher (interaction term $F = 4.272$, $p = 0.026$) in SI + V (0.134 ± 0.0137 nmol/mg) and repeated SI R–SI + V (0.143 ± 0.015) vs G + V (0.0402 ± 0.0125 nmol/mg). The detected level of H_2O_2 was significantly lower in SI + D (0.0803 ± 0.0177) and R–SI + D (0.083 ± 0.0177) following DHM 2 mg/kg treatment (Fig. 2A). Additionally, this observation was consistent even after a period of SI stress discontinuation followed by repeated SI.

ROS are produced in the mitochondria at various locations on the electron transport chain (ETC), complex proteins necessary for mitochondrial respiration (Indo et al., 2007). Because stress is known to play a role in ROS production, protein levels were analyzed in the five mitochondrial complexes that comprise the ETC (Zlatković and Filipović, 2013). Significant reductions in the expression (interaction term $F = 2.273$, $p = 0.03$) of C–I (0.574 ± 0.035), C-II (0.440 ± 0.098), and C-IV (0.503 ± 0.129) were identified in SI + V compared to the control G + V C–I (1.116 ± 0.115), C-II (0.851 ± 0.116), and C-IV (1.052 ± 0.152). DHM treatment restored the protein expressions of C–I (0.983 ± 0.139), C-II (0.780 ± 0.098), and C-IV (1.036 ± 0.120) in SI + D group relative to the SI + V (Fig. 2C, D, F). SI did not influence the protein expressions of C-III and C–V (Fig. 2E, G).

To examine the functional impact of the reduction of these protein levels, we performed a colorimetric complex activity assay on complexes I, II, and IV. Activities were significantly reduced in all three complexes of SI + V, C–I ($F = 2.273$, $p = 0.03$) (5.152 ± 1.010), C-II ($F = 6.151$, $p = 0.021$) (1.416 ± 0.1435), and C-IV ($F = 3.679$, $p = 0.03$) (2.203 ± 0.6186), compared to the controls G + V, C–I (15.62 ± 0.9292), C-II (4.002 ± 0.5492), and C-IV (8.832 ± 1.780) (Fig. 3). DHM restored the function of C–I (13.79 ± 3.576) and C-IV (7.246 ± 1.427), but not quite in C-II (2.850 ± 0.3758) (Fig. 3B).

3.2. Social isolation and repeated social isolation enhance the activities of mitochondrial antioxidative enzymes, while DHM normalizes them

The activity and protein levels of the mitochondrial antioxidant enzymes superoxide dismutase 2 (SOD2), heme oxygenase-1 (HO-1), peroxiredoxin-3 (PRDX3), and glutathione peroxidase 4 (GPX4) were measured to determine the effects of SI and DHM on the mitochondria's antioxidant defense system. Superoxide anions (O_2^-) are a byproduct of phosphorylation that can damage the ETC and other components of the mitochondria. All four proteins are involved in the protection from or response to oxidative stress. SOD2 converts superoxide radicals into less reactive H_2O_2 molecules, preventing further damage (Storz et al., 2005). HO-1 is an enzyme that has been implicated in the regulation of stress and the cell's adaptive response to oxidative injury (Chen et al., 2000). PRDX3 prevents ROS from harming the mitochondria by efficiently removing H_2O_2 from the mitochondrial matrix (Chen et al., 2008). GPX4 is a part of the glutathione redox cycle, which is an important line of defense against H_2O_2 and lipid hydroperoxides (Imai and Nakagawa, 2003; Ran et al., 2006). Colorimetric analyses and Western blot were used to determine the activity and protein ratios, respectively. The activity of total SOD enzyme in SI + V ($F = 5.384$, $p = 0.011$) (106.9 ± 5.93, $p = 0.002$) was substantially higher than G + V (83.88 ± 5.76). DHM treatment (SI + D) reduced the level of total SOD to 75.90 ± 7.66 (Fig. 4C). Additionally, the protein expression of antioxidant enzymes SOD2 ($F = 5.384$, $p = 0.01$) (1.787 ± 0.188), HO-1 ($F = 3.727$, $p = 0.03$)

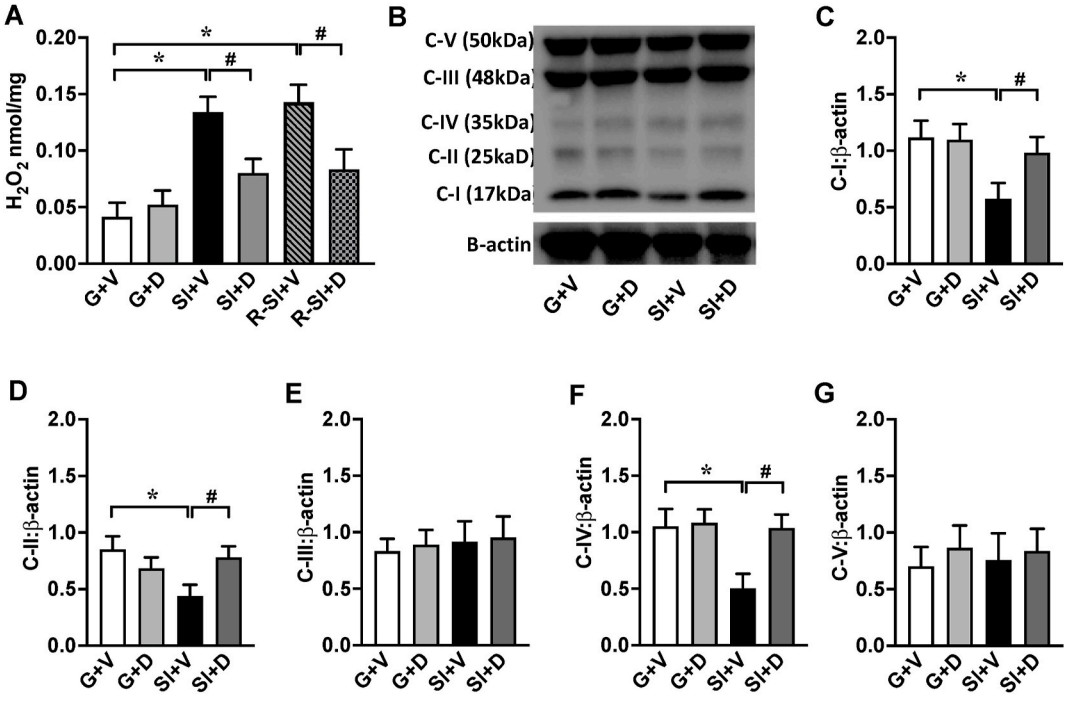

Fig. 2. SI mice exhibit an increase in H_2O_2 Levels and a decrease in mitochondrial complexes I, II, and IV, while DHM normalizes them. (A) The levels of H_2O_2 nmol/mg of PFC tissue after 4 weeks of SI (SI + V), repeated SI (R–SI + V), and after DHM treatment (SI + D, R–SI + D). **(B)** Representative Western blots of OxPhos proteins expression in ETC C–V (50 kDa), C-III (48 kDa), C-IV (35 kDa), C-II (25 kDa), C–I (17 kDa), and β-actin (42 kDa). **(C, D, E, F, and G)** Quantitative analysis ratio of C–I, C-II, C-III, C-IV, and C–V. Values were normalized by the corresponding β-actin. Data are presented as mean ± SEM values (n = 4–6 for A, n = 7 for C, D, E, F, and G). Two-way ANOVA followed by multiple comparisons, Holm-Sidak's method *$p < 0.05$ vs. G + V, #$p < 0.05$ vs. SI + V or R–SI + V.

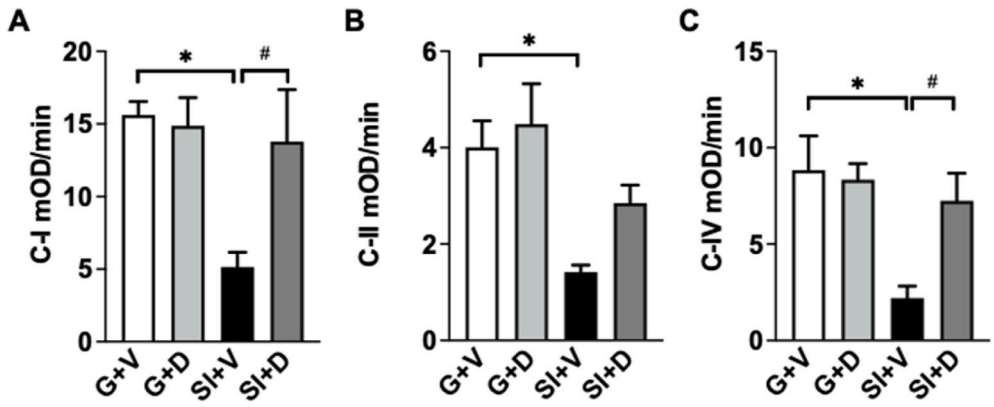

Fig. 3. SI mice exhibit a decreased function in mitochondrial complexes I, II, and IV, while DHM normalizes complex I and IV function. Function of C–I (**A**), C-II (**B**), and C-IV (**C**) in ETC reported as the change in mOD/min based on a colorimetric assay. Data are presented as mean ± SEM values (n = 6). Two-way ANOVA followed by multiple comparisons, Holm-Sidak method. *$p \leq 0.05$, vs G + V, #$p \leq 0.05$ vs SI + V.

(1.584 ± 0.154), and GPX4 (F = 5.911, p = 0.006) (1.754 ± 0.184) were significantly higher in SI + V compared to the control (G + V). DHM treatment after SI (SI + D) showed protein expression levels similar to the control: SOD2 (1.218 ± 0.163), HO-1(1.282 ± 0.154), PRDX3 (1.28 ± 0.354), and GPX4 (1.185 ± 0.184) (not statistically different from G + V group). The G + D group showed a significant increase compared to G + V for SOD2 (1.398 ± 0.115), HO-1 (1.316 ± 0.109), and GPX4 (1.409 ± 0.130), except PRDX3 (1.56 ± 0.26) did not show the difference (Fig. 4D, E, F, and G). Furthermore, the level of PRDX3 (2.047 ± 0.364) and GPX4 (1.675 ± 0.184) in R–SI + V was upregulated after repeated SI compared to the control. Meanwhile, the levels of HO-1 (1.088 ± 0.169), PRDX3 (1.672 ± 0.364), and GPX4 (1.292 ± 0.184) in R–SI + D group showed similar protein expression to the control G + V group (Fig. 4E, F, G). SOD2 expression level did not change among all treatment groups after repeated SI (Fig. 4D).

3.3. Social isolation and repeated social isolation affect Bcl-1 and p62 protein expression, while DHM normalizes them

Beclin-1 (Bcl-1) and sequestosome 1 (SQSTM1/p62) are involved in the autophagy mitochondrial-dependent apoptosis pathway that is activated in response to ROS and oxidative insults (Shefa et al., 2019). Therefore, we assessed the protein expression of Bcl-1 and p62 after SI and repeated SI. The level of Bcl-1 (1.072 ± 0.121) after SI did not show a reduction, yet p62 (F = 1.727, p = 0.004) (0.704 ± 0.083) demonstrates a reduction compared to G + V (0.978 ± 0.083). Furthermore, the protein expressions of Bcl-1 (F = 6.970, p = 0.004) (0.493 ± 0.135) and p62 (F = 6.126, p = 0.006) (0.65 ± 0.083) in R–SI + V were decreased compared to the group-housed (G + V). Administration of DHM after repeated SI (R–SI + D) restored the level of p62 (0.955 ± 0.083) (Fig. 5D).

3.4. Social isolation and repeated social isolation modulate BDNF-TrkB signaling pathway, while DHM improves them

BDNF plays a crucial role in neuroprotection via activation of tropomyosin-related kinase B (TrkB) receptor (Ji et al., 2016). Once BDNF binds to its receptor, TrkB, several transcriptional cascades are activated, including the extracellular signal-regulated MAP kinase (Erk1/2) pathway (Mao et al., 2015). BDNF has also been shown to increase neuronal mitochondrial respiration through complex I enhancement, via the MAP kinase pathway (Mattson, 2007). To explore the effect of SI on neuronal mediators, the protein levels of BDNF, TrkB, and Erk1/2 in PFC homogenates were measured using ELISA and Western blot. The results revealed that SI and repeated SI induced a significant reduction in the BDNF levels in SI + V (F = 5.457, p = 0.048) (4.844 ± 0.112 pg/mg) relative to G + V (5.711 ± 0.105 pg/mg). DHM treatment reversed this effect in SI + D (5.743 ± 0.119 pg/mg). The BDNF normalized to β-actin in R–SI + V was 0.657 ± 0.114 vs. the control G + V (set as 1) (Fig. 6C and D). DHM treatment reversed this effect in R–SI + D (1.058 ± 0.242). Additionally, the normalized phosphorylated TrkB (p-TrkB) protein expression reduced after repeated SI (F = 1.614, p = 0.001) (0.607 ± 0.146). DHM treatment restored the level of p-TrkB in SI + D (1.128 ± 0.158) and in R–SI + D (1.028 ± 0.127) (Fig. 6E). SI induced a reduction in normalized phosphorylated Erk p42 (p-Erk p42) (F = 1.078, p = 0.03) (0.663 ± 0.109) and phosphorylated Erk p44 (p-Erk p44) (F = 3.164, p = 0.05) (0.452 ± 0.146) in SI + V, while DHM treatment (SI + D) improved p-Erk p42 (1.133 ± 0.102) and p-Erk p44 (1.310 ± 0.146) protein expression (Fig. 6G and I). The protein expression of p-Erk p42 (0.831 ± 0.116) and p-Erk p44 (0.761 ± 0.164) after repeated SI (R–SI + V) were slightly decreased (Fig. 6G and I).

4. Discussion

Social isolation is considered a common psychological stressor, inducing pathological changes in the neuroendocrine system, immune system, neurotrophic factors, and mitochondrial functions (Mumtaz et al., 2018; Murínová et al., 2017; Chan et al., 2017; Calcia et al., 2016; Möller et al., 2013). In the present study, we demonstrated that short-term SI disrupted mitochondrial activity through reduction and impairment in C–I, C-II, and C-IV in the ETC. Additionally, SI increased ROS and several mitochondrial antioxidative enzymes, including SOD2, HO-1, PRDX-3, and GPX4. Moreover, disbalance in the autophagy processes and the BDNF-TrkB pathway were attributed to SI. We also found that repeated SI induced equivalent effects on ROS production, antioxidative enzymes, autophagy, and the BDNF-TrkB pathway.

ROS is the downstream product of mitochondrial energy production and plays an essential role in cellular homeostasis under normal physiological conditions (Schieber and Chandel, 2014; Diebold and Chandel, 2016). Under stressful conditions, however, ETC subunits undergo disruption resulting in ROS accumulation that leads to oxidative stress damage (Andreazza et al., 2010; Xing et al., 2013). ROS accumulation contributes to the prolonged activation of microglia and astrocytes, causing persistent neuroinflammation, further ROS production, and additional oxidative damage (Wang et al., 2004, 2018). This statement is consistent with our previous findings, where short-term SI induced overactivated microglia and reduced astrocyte plasticity (Al Omran et al., 2022; Watanabe et al., 2022). Eventually, this series of events drive alterations to synaptic plasticity and neurotransmission activities, particularly the GABAergic system, which eventually result in multiple behavioral deficits and anxiety disorders. Reflective of this pathway, our

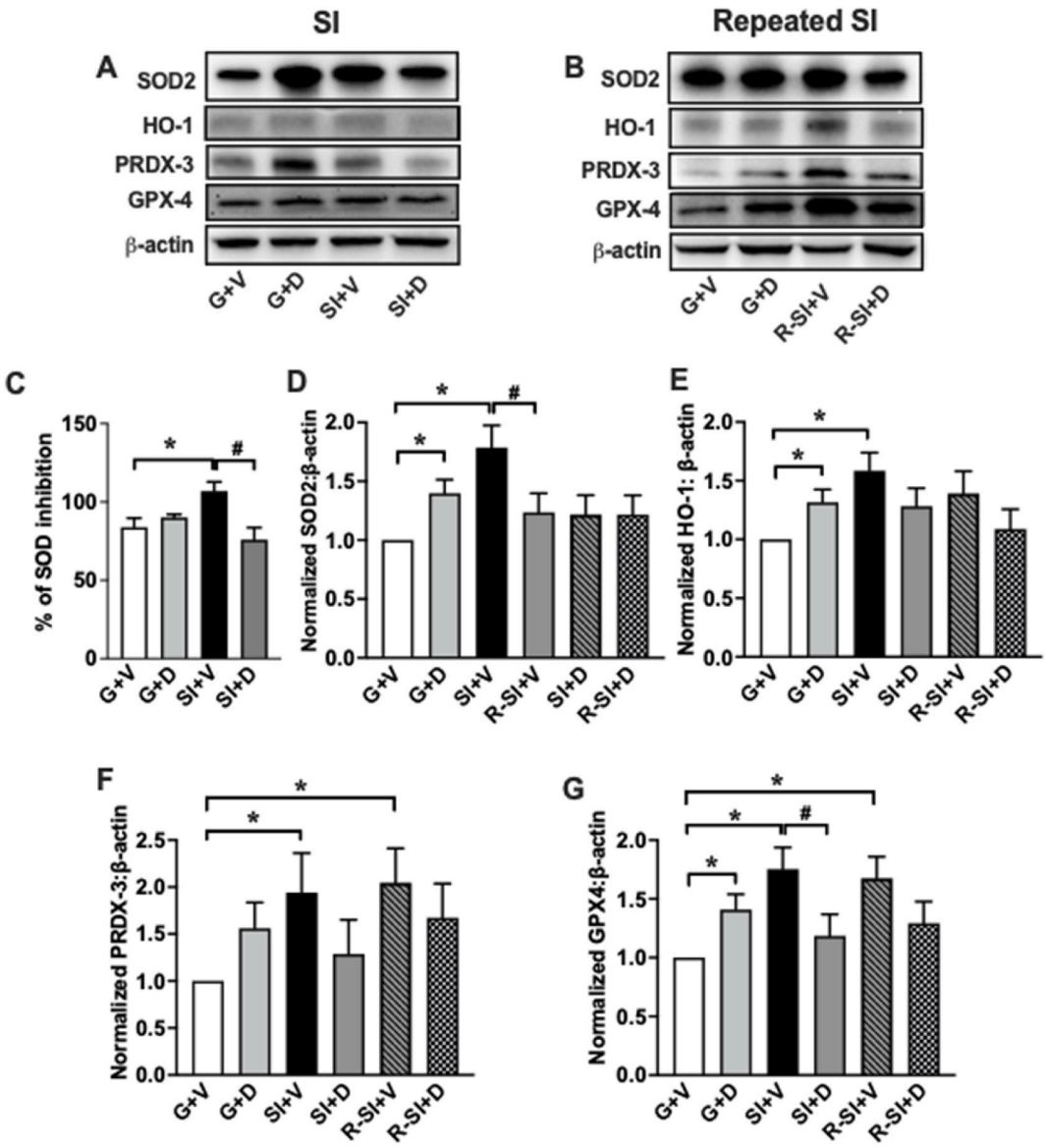

Fig. 4. Modulation of mitochondrial antioxidant enzymes activity and protein levels induced by SI, repeated SI, and DHM treatment. (A, B) Representative Western blot of proteins expression of SOD2, HO-1, PRDX-3, GPX4, and β -actin. **(C)** Total SOD activity is represented as percent inhibition of H_2O_2. **(D, E, F, and G)** SOD2, HO-1, PRDX-3, and GPX4 antioxidant capacity were detected by measuring the protein expression of each antioxidant enzyme using western blot, and the values were normalized by the corresponding β-actin. Data in D-G are normalized to G + V and presented as the mean ± SEM. Two-way ANOVA followed by multiple comparisons, Holm-Sidak's method $*p < 0.05$ vs. G + V, $\#p < 0.05$ vs. SI + V or R–SI + V.

previous study found impaired GABAergic transmission in SI mice (Silva et al., 2020). Considering this causative relation between neuroinflammation and mitochondrial viability, we assessed the level of ROS production after SI and repeated SI. Our results indicated a significant increase in H_2O_2 levels in SI and repeated SI (Fig. 3A). Several studies strongly suggested that the level of ROS production is an indicator of mitochondrial impairment in the SI anxiety model (Shao et al., 2015; Todorović et al., 2016). Combined with our previous findings, SI-induced anxiety is a cycle of ROS accumulation, ETC disruption, persistent neuroinflammation, and GABAergic impairment.

Mitochondria play a predominant role in ATP production, intercellular calcium signaling, and ROS production and elimination balance. These functions are essential in sustaining and executing the complex functions of neurotransmission and synaptic plasticity (Obashi and Okabe, 2013; Billups and Forsythe, 2002; Chang et al., 2006). Mitochondrial protein complexes that constitute the ETC are vital to mitochondrial energy production through oxidative phosphorylation (OXPHOS). The viability of the complexes in the ETC is a major indicator of mitochondrial functionality (Indo et al., 2007). We evaluated the protein expression of mitochondria complexes after SI and found a reduction in C–I, C-II, and C-IV protein expression (Fig. 2C, D, F) and function (Fig. 3). This finding is consistent with other studies that showed different anxiety animal models exhibit an impairment in C–I, C-II, and C-IV functions (Hollis et al., 2015; Perić et al., 2018; Gebara et al., 2021). ETC subunit disruptions contribute to the pathology of neuropsychiatric and neurodegenerative disorders such as anxiety, depression, PTSD, and dementia (Rammal et al., 2008; Sarandol et al., 2007; Tezcan et al., 2003). DHM was able to restore C–I, C-II, and C-IV expression and C–I and C-IV function (Fig. 2C, D, F and Fig. 3A, C). Restoration of C-II expression but not function warrants further investigation. Though speculative, two weeks of DHM may not have been enough time for C-II function to recover. Overall, these results suggest that DHM has pharmacotherapeutic effects on C–I and C-IV, which subsequently improves ROS levels in the PFC.

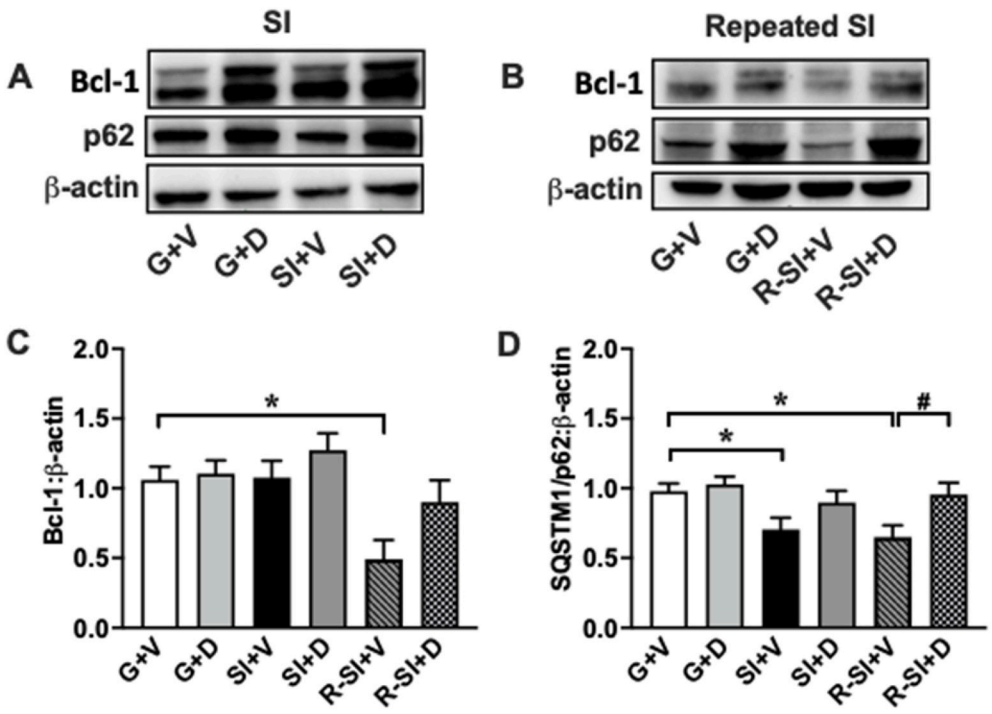

Fig. 5. Modulation of Bcl-1 and SQSTM1/p62 after SI, repeated SI, and DHM treatment. (A, B) Representative blots of Bcl-1 and SQSTM1/p62 after 4 weeks of SI and repeated SI and 2 weeks of DHM treatment, 2 mg/kg **(C, D)** Quantified relative values of protein expression of Bcl-1 and SQSTM1/p62 after SI, repeated SI, and 2 weeks of DHM 2 mg/kg β-actin was used as a loading control. Data are presented as the mean ± SEM (n = 4–7). Two-way ANOVA followed by multiple comparisons, Holm-Sidak's method $*p < 0.05$ vs. G + V, $\#p < 0.05$ vs. SI + V or R–SI + V.

Mitochondria also produce several antioxidative enzymes to eliminate the harmful ROS, such as SOD2, HO-1, PRDX-3, and GPX4 (Hollis et al., 2015; Filipović et al., 2017). The levels of antioxidative enzymes are a distinct indicator of mitochondrial viability. Our results indicated increases in total SOD activity and SOD2 protein expression following SI (Fig. 4C and D). This increase was normalized by DHM treatment to a level relevant to the control. The SOD2 activity and protein expression in SI was closer to DHM treated group-housed, which potentially suggests a stress compensation mechanism. Our present data are consistent with several studies of SI-induced anxiety that showed an increase in SOD activity after SI (Krolow et al., 2012). SI and repeated SI also enhanced the expression of HO-1, PRDX-3, and GPX4, while DHM treatment reversed these effects (Fig. 4E, F, G). Combined, our results indicate that SI correlates with an increase in antioxidant activity protein expression as a compensatory mechanism, while DHM has a pharmacologic effect on normalizing these levels by reducing overall oxidative stress.

Autophagy is a vital process of selective degradation of cellular components. In the central nervous system (CNS), autophagy sustains neuronal integrity and maintains neuroplasticity via regulating the clustering of synaptic vesicles and facilitating synaptic pruning (Nikoletopoulou et al., 2017). Therefore, autophagy dysregulation has been proposed to be associated with various neuropsychological disorders (Pierone et al., 2020). At the cellular level, proper mitophagy, a process essential for mitochondria quality control in the CNS, is essential to prevent ROS accumulation by eliminating the cytosolic mitochondrial DNA (Nakahira et al., 2011). Downregulation of autophagy-related proteins such as Bcl-1 and SQSTM1/p62 has been associated with impairment of autophagy/mitophagy and, ultimately, development of behavioral deficits (Geng et al., 2019). In the current study, social isolation for four weeks did not show a significant difference in Bcl-1, but a reduction in p62 was observed. However, repeated SI induced downregulation of both Bcl-1 and p62 (Fig. 5). DHM treatment alleviated the reduction of Bcl-1 and p62 protein expression and restored autophagy. This finding is consistent with multiple studies that showed a reduction in Bcl-1 and p62 in stress-related models (Geng et al., 2019; Zheng et al., 2017; Yang et al., 2017; Wang et al., 2019; Einat et al., 2005). Collectively, these results indicated that autophagy functionality decreased progressively after multiple SI episodes. This reduction contributes to insufficient mitophagy, resulting in increased oxidative stress. Two weeks of DHM treatment counteracted these changes.

Several preclinical and clinical studies have demonstrated a causal relationship between BNDF dysfunction and anxiety, depression, and cognitive behaviors (Suliman et al., 2013; Ieraci et al., 2016). Importantly, BDNF responds to increased energy demands by enhancing mitochondrial respiratory coupling at complex I (Mattson et al., 2008). The present study demonstrated a reduction in the PFC BDNF-TrkB pathway and p-Erk1/2 expression following SI and repeated SI (Fig. 6). This reduction was improved by DHM administration. These findings suggest that mitochondrial complex dysfunction is related to BDNF reduction, where respiratory coupling is impaired at complex I. DHM restores BDNF levels and thereby restores C–I function. The exact relationship between BDNF reduction, downstream pathway, and ETC disruption is of interest for further investigation.

One limitation of the current study is that the number of mice in repeated SI groups was low. Therefore, despite the trend of reduction in antioxidative enzymes and p-Erk1/2 that was observed, the power was not deemed high enough to promote statistical significance. Further studies looking at other anxiety-related brain regions, such as the hippocampus and amygdala, are necessary to analyze the connections between these regions and further verify the therapeutic effect of DHM. Moreover, while we found several effects of DHM on SI-induced anxiety, based on this study, we cannot pinpoint where DHM majorly acts. Future studies will incorporate inhibitors or knockout models to investigate the root target of DHM as well as the mechanism of SI-induced anxiety. As this study only included male mice, future studies will also incorporate female mice.

Overall, the current results suggest that DHM produces its anxiolytic effects by modulating the function of mitochondria, reducing oxidative stress, maintaining antioxidant levels, normalizing autophagy, and enhancing BDNF. Additionally, since DHM counteracts the impact of repeated social isolation stress, our findings suggest that DHM can provide long-term protection against stress-induced CNS impairment and behavioral consequences. Combined with our previous findings that DHM counteracts neuroinflammatory effects (Al Omran et al., 2022; Watanabe et al., 2022), DHM acts as a neuroprotective agent by modulating the glial-mitochondrial pathway and therefore restoring

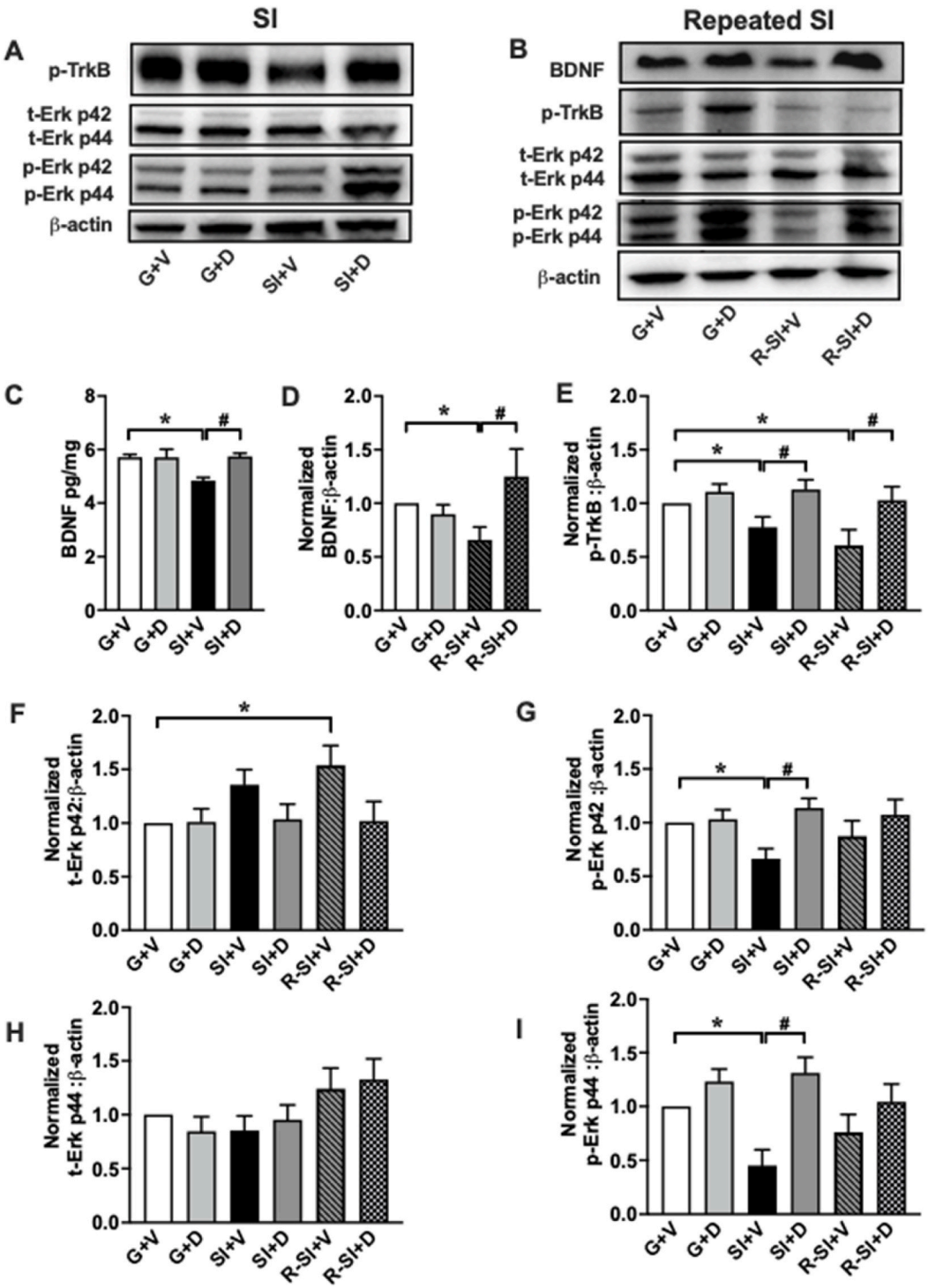

Fig. 6. Reduction of BNDF, p-TrkB, p-Erk p42, and p-Erk p44 protein levels after SI and repeated SI; DHM improves them. (A, B) Representative blots of BDNF, p-TrkB, t-Erk p42, p-Erk p42, t-Erk p44, and p-Erk p44. **(C)** Quantitative measurement of BDNF protein levels after SI and 2 mg/kg DHM treatment in PFC homogenates using ELISA. **(D, E, F, G, H, and I)** Quantified the relative values of protein expression of BDNF after repeated SI along with p-TrkB, t-Erk p42, p-Erk p42, t-Erk p44, and p-Erk p44 values after SI, repeated SI, and 2 weeks of DHM 2 mg/kg treatment. β-actin was used as a loading control and data in E-I are normalized to G + V. Data are presented as the mean ± SEM (n = 4–7). Two-way ANOVA followed by multiple comparisons, Holm-Sidak's method *$p < 0.05$ vs. G + V, #$p < 0.05$ vs. SI + V or R–SI + V.

GABAergic neurotransmission. It would be of interest to identify whether DHM reduces neuroinflammation by restoring ETC function or, vice versa, restores ETC function by reducing neuroinflammation. Exploring this question will also shed light on the pathophysiology of anxiety.

Funding and disclosure

USC Good-Neighbor and Carefree Biotechnology Foundations (to J. L), Saudi Arabian Cultural Mission (to A.J.A), and R01HL135623 and NIDA R42DA044788 (to X. M. S). The authors have nothing to disclose.

CRediT authorship contribution statement

Alzahra J. Al Omran: Formal analysis, Data curation, Writing – original draft, designed and performed experiments, analyzed data, generated figures, and wrote the manuscript. **Saki Watanabe:** Formal analysis, Data curation, Writing – original draft, discussed the design, performed experiments, analyzed data, generated figures, and wrote the manuscript. **Ethan C. Hong:** Formal analysis, Data curation, Writing – original draft, performed experiments, analyzed data, and wrote the manuscript. **Samantha G. Skinner:** Formal analysis, Data curation, Writing – original draft, performed experiments, analyzed data, and wrote the manuscript. **Mindy Zhang:** Formal analysis, Data curation, Writing – original draft, performed experiments, analyzed data, and wrote the manuscript. **Jifeng Zhang:** Formal analysis, Data curation, performed experiments and analyzed data. **Xuesi M. Shao:** Formal analysis, Writing – original draft, discussed the design of experiments, statistical analyses, and wrote the manuscript. **Jing Liang:** Formal analysis, Writing – original draft, Supervision, established animal model, designed experiments, statistical analyses, wrote the manuscript and supervised the project.

Declaration of interest

The authors have nothing to disclose.

Data availability

Data will be made available on request.

Acknowledgments

We thank N. Kirmiz for manuscript editing.

References

Al Omran, A.J., Shao, A.S., Watanabe, S., Zhang, Z., Zhang, J., Xue, C., et al., 2022. Social isolation induces neuroinflammation and microglia overactivation, while dihydromyricetin prevents and improves them. J. Neuroinflammation 19 (1), 2.

Andreazza, A.C., Andersen, M.L., Alvarenga, T.A., de-Oliveira, M.R., Armani, F., Ruiz, F. S., et al., 2010. Impairment of the mitochondrial electron transport chain due to sleep deprivation in mice. J. Psychiatr. Res. 44 (12), 775–780.

Banagozar Mohammadi, A., Torbati, M., Farajdokht, F., Sadigh-Eteghad, S., Fazljou, S.M. B., Vatandoust, S.M., et al., 2019. Sericin alleviates restraint stress induced depressive- and anxiety-like behaviors via modulation of oxidative stress, neuroinflammation and apoptosis in the prefrontal cortex and hippocampus. Brain Res. 1715, 47–56.

Becker, E., Orellana Rios, C.L., Lahmann, C., Rücker, G., Bauer, J., Boeker, M., 2018. Anxiety as a risk factor of Alzheimer's disease and vascular dementia. Br. J. Psychiatry 213 (5), 654–660.

Beutel, M.E., Klein, E.M., Brähler, E., Reiner, I., Jünger, C., Michal, M., et al., 2017. Loneliness in the general population: prevalence, determinants and relations to mental health. BMC Psychiatr. 17 (1), 97.

Billups, B., Forsythe, I.D., 2002. Presynaptic mitochondrial calcium sequestration influences transmission at mammalian central synapses. J. Neurosci. 22 (14), 5840–5847.

Burgos-Robles, A., Vidal-Gonzalez, I., Quirk, G.J., 2009. Sustained conditioned responses in prelimbic prefrontal neurons are correlated with fear expression and extinction failure. J. Neurosci. 29 (26), 8474–8482.

Calcia, M.A., Bonsall, D.R., Bloomfield, P.S., Selvaraj, S., Barichello, T., Howes, O.D., 2016. Stress and neuroinflammation: a systematic review of the effects of stress on microglia and the implications for mental illness. Psychopharmacology (Berl) 233 (9), 1637–1650.

Chan, J.N., Lee, J.C., Lee, S.S., Hui, K.K., Chan, A.H., Fung, T.K., et al., 2017. Interaction effect of social isolation and high dose corticosteroid on neurogenesis and emotional behavior. Front. Behav. Neurosci. 11, 18.

Chanana, P., Kumar, A., 2016. GABA-BZD receptor modulating mechanism of panax quinquefolius against 72-h sleep deprivation induced anxiety like behavior: possible roles of oxidative stress, mitochondrial dysfunction and neuroinflammation. Front. Neurosci. 10, 84.

Chang, D.T., Honick, A.S., Reynolds, I.J., 2006. Mitochondrial trafficking to synapses in cultured primary cortical neurons. J. Neurosci. 26 (26), 7035–7045.

Chen, K., Gunter, K., Maines, M.D., 2000. Neurons overexpressing heme oxygenase-1 resist oxidative stress-mediated cell death. J. Neurochem. 75 (1), 304–313.

Chen, L., Na, R., Gu, M., Salmon, A.B., Liu, Y., Liang, H., et al., 2008. Reduction of mitochondrial H2O2 by overexpressing peroxiredoxin 3 improves glucose tolerance in mice. Aging Cell 7 (6), 866–878.

Collaborators, C.-M.D., 2021. Global prevalence and burden of depressive and anxiety disorders in 204 countries and territories in 2020 due to the COVID-19 pandemic. Lancet 398 (10312), 1700–1712.

Diebold, L., Chandel, N.S., 2016. Mitochondrial ROS regulation of proliferating cells. Free Radic. Biol. Med. 100, 86–93.

Einat, H., Yuan, P., Manji, H.K., 2005. Increased anxiety-like behaviors and mitochondrial dysfunction in mice with targeted mutation of the Bcl-2 gene: further support for the involvement of mitochondrial function in anxiety disorders. Behav. Brain Res. 165 (2), 172–180.

Facts and Statistics, 2016. Anxiety and depression association of America [Internet]. https://adaa.org/understanding-anxiety/facts-statistics.

Filipović, D., Todorović, N., Bernardi, R.E., Gass, P., 2017. Oxidative and nitrosative stress pathways in the brain of socially isolated adult male rats demonstrating depressive- and anxiety-like symptoms. Brain Struct. Funct. 222 (1), 1–20.

Gebara, E., Zanoletti, O., Ghosal, S., Grosse, J., Schneider, B.L., Knott, G., et al., 2021. Mitofusin-2 in the nucleus accumbens regulates anxiety and depression-like behaviors through mitochondrial and neuronal actions. Biol. Psychiatr. 89 (11), 1033–1044.

Geng, J., Liu, J., Yuan, X., Liu, W., Guo, W., 2019. Andrographolide triggers autophagy-mediated inflammation inhibition and attenuates chronic unpredictable mild stress (CUMS)-induced depressive-like behavior in mice. Toxicol. Appl. Pharmacol. 379, 114688.

Hettema, J.M., Prescott, C.A., Myers, J.M., Neale, M.C., Kendler, K.S., 2005. The structure of genetic and environmental risk factors for anxiety disorders in men and women. Arch. Gen. Psychiatr. 62 (2), 182–189.

Hollis, F., van der Kooij, M.A., Zanoletti, O., Lozano, L., Cantó, C., Sandi, C., 2015. Mitochondrial function in the brain links anxiety with social subordination. Proc. Natl. Acad. Sci. U. S. A. 112 (50), 15486–15491.

Hou, X., Tong, Q., Wang, W., Xiong, W., Shi, C., Fang, J., 2015. Dihydromyricetin protects endothelial cells from hydrogen peroxide-induced oxidative stress damage by regulating mitochondrial pathways. Life Sci. 130, 38–46.

Ieraci, A., Mallei, A., Popoli, M., 2016. Social isolation stress induces anxious-depressive-like behavior and alterations of neuroplasticity-related genes in adult male mice. Neural Plast. 2016, 6212983.

Imai, H., Nakagawa, Y., 2003. Biological significance of phospholipid hydroperoxide glutathione peroxidase (PHGPx, GPx4) in mammalian cells. Free Radic. Biol. Med. 34 (2), 145–169.

Indo, H.P., Davidson, M., Yen, H.C., Suenaga, S., Tomita, K., Nishii, T., et al., 2007. Evidence of ROS generation by mitochondria in cells with impaired electron transport chain and mitochondrial DNA damage. Mitochondrion 7 (1–2), 106–118.

Ji, L.L., Peng, J.B., Fu, C.H., Cao, D., Li, D., Tong, L., et al., 2016. Activation of Sigma-1 receptor ameliorates anxiety-like behavior and cognitive impairments in a rat model of post-traumatic stress disorder. Behav. Brain Res. 311, 408–415.

Kessler, R.C., Birnbaum, H.G., Shahly, V., Bromet, E., Hwang, I., McLaughlin, K.A., et al., 2010. Age differences in the prevalence and co-morbidity of DSM-IV major depressive episodes: results from the WHO World Mental Health Survey Initiative. Depress. Anxiety 27 (4), 351–364.

Klinenberg, E., 2016. Social isolation, loneliness, and living alone: identifying the risks for public health. Am. J. Publ. Health 106 (5), 786–787.

Krolow, R., Noschang, C., Weis, S.N., Pettenuzzo, L.F., Huffell, A.P., Arcego, D.M., et al., 2012. Isolation stress during the prepubertal period in rats induces long-lasting neurochemical changes in the prefrontal cortex. Neurochem. Res. 37 (5), 1063–1073.

Li, C., Li, M., Yu, H., Shen, X., Wang, J., Sun, X., et al., 2017. Neuropeptide VGF C-terminal peptide TLQP-62 alleviates lipopolysaccharide-induced memory deficits and anxiety-like and depression-like behaviors in mice: the role of BDNF/TrkB signaling. ACS Chem. Neurosci. 8 (9), 2005–2018.

Liang, J., López-Valdés, H.E., Martínez-Coria, H., Lindemeyer, A.K., Shen, Y., Shao, X.M., et al., 2014. Dihydromyricetin ameliorates behavioral deficits and reverses neuropathology of transgenic mouse models of Alzheimer's disease. Neurochem. Res. 39 (6), 1171–1181.

Loades, M.E., Chatburn, E., Higson-Sweeney, N., Reynolds, S., Shafran, R., Brigden, A., et al., 2020. Rapid systematic review: the impact of social isolation and loneliness on the mental health of children and adolescents in the context of COVID-19. J. Am. Acad. Child Adolesc. Psychiatry 59 (11), 1218–1239 e3.

Mao, X.Y., Cao, Y.G., Ji, Z., Zhou, H.H., Liu, Z.Q., Sun, H.L., 2015. Topiramate protects against glutamate excitotoxicity via activating BDNF/TrkB-dependent ERK pathway in rodent hippocampal neurons. Prog. Neuro-Psychopharmacol. Biol. Psychiatry 60, 11–17.

Mattson, M.P., 2007. Mitochondrial regulation of neuronal plasticity. Neurochem. Res. 32 (4–5), 707–715.

Mattson, M.P., Gleichmann, M., Cheng, A., 2008. Mitochondria in neuroplasticity and neurological disorders. Neuron 60 (5), 748–766.

Möller, M., Du Preez, J.L., Viljoen, F.P., Berk, M., Emsley, R., Harvey, B.H., 2013. Social isolation rearing induces mitochondrial, immunological, neurochemical and behavioural deficits in rats, and is reversed by clozapine or N-acetyl cysteine. Brain Behav. Immun. 30, 156–167.

Mumtaz, F., Khan, M.I., Zubair, M., Dehpour, A.R., 2018. Neurobiology and consequences of social isolation stress in animal model-A comprehensive review. Biomed. Pharmacother. 105, 1205–1222.

Murínová, J., Hlaváčová, N., Chmelová, M., Riečanský, I., 2017. The evidence for altered BDNF expression in the brain of rats reared or housed in social isolation: a systematic review. Front. Behav. Neurosci. 11, 101.

Nakahira, K., Haspel, J.A., Rathinam, V.A., Lee, S.J., Dolinay, T., Lam, H.C., et al., 2011. Autophagy proteins regulate innate immune responses by inhibiting the release of mitochondrial DNA mediated by the NALP3 inflammasome. Nat. Immunol. 12 (3), 222–230.

Nikoletopoulou, V., Sidiropoulou, K., Kallergi, E., Dalezios, Y., Tavernarakis, N., 2017. Modulation of autophagy by BDNF underlies synaptic plasticity. Cell Metabol. 26 (1), 230–242 e5.

Nugent, N.R., Tyrka, A.R., Carpenter, L.L., Price, L.H., 2011. Gene-environment interactions: early life stress and risk for depressive and anxiety disorders. Psychopharmacology (Berl) 214 (1), 175–196.

Nuss, P., 2015. Anxiety disorders and GABA neurotransmission: a disturbance of modulation. Neuropsychiatric Dis. Treat. 11, 165–175.

Obashi, K., Okabe, S., 2013. Regulation of mitochondrial dynamics and distribution by synapse position and neuronal activity in the axon. Eur. J. Neurosci. 38 (3), 2350–2363.

Perić, I., Costina, V., Stanisavljević, A., Findeisen, P., Filipović, D., 2018. Proteomic characterization of hippocampus of chronically socially isolated rats treated with fluoxetine: depression-like behaviour and fluoxetine mechanism of action. Neuropharmacology 135, 268–283.

Pierone, B.C., Pereira, C.A., Garcez, M.L., Kaster, M.P., 2020. Stress and signaling pathways regulating autophagy: from behavioral models to psychiatric disorders. Exp. Neurol. 334, 113485.

Rammal, H., Bouayed, J., Younos, C., Soulimani, R., 2008. Evidence that oxidative stress is linked to anxiety-related behaviour in mice. Brain Behav. Immun. 22 (8), 1156–1159.

Ran, Q., Gu, M., Van Remmen, H., Strong, R., Roberts, J.L., Richardson, A., 2006. Glutathione peroxidase 4 protects cortical neurons from oxidative injury and amyloid toxicity. J. Neurosci. Res. 84 (1), 202–208.

Roy-Byrne, P., 2015. Treatment-refractory anxiety; definition, risk factors, and treatment challenges. Dialogues Clin. Neurosci. 17 (2), 191–206.

Sarandol, A., Sarandol, E., Eker, S.S., Erdinc, S., Vatansever, E., Kirli, S., 2007. Major depressive disorder is accompanied with oxidative stress: short-term antidepressant treatment does not alter oxidative-antioxidative systems. Hum. Psychopharmacol. 22 (2), 67–73.

Schieber, M., Chandel, N.S., 2014. ROS function in redox signaling and oxidative stress. Curr. Biol. 24 (10), R453–R462.

Shao, Y., Yan, G., Xuan, Y., Peng, H., Huang, Q.J., Wu, R., et al., 2015. Chronic social isolation decreases glutamate and glutamine levels and induces oxidative stress in the rat hippocampus. Behav. Brain Res. 282, 201–208.

Shefa, U., Jeong, N.Y., Song, I.O., Chung, H.J., Kim, D., Jung, J., et al., 2019. Mitophagy links oxidative stress conditions and neurodegenerative diseases. Neural Regen Res 14 (5), 749–756.

Shen, Y., Lindemeyer, A.K., Gonzalez, C., Shao, X.M., Spigelman, I., Olsen, R.W., et al., 2012. Dihydromyricetin as a novel anti-alcohol intoxication medication. J. Neurosci. 32 (1), 390–401.

Silva, J., Shao, A.S., Shen, Y., Davies, D.L., Olsen, R.W., Holschneider, D.P., et al., 2020. Modulation of hippocampal GABAergic neurotransmission and gephyrin levels by dihydromyricetin improves anxiety. Front. Pharmacol. 11, 1008.

Storz, P., Döppler, H., Toker, A., 2005. Protein kinase D mediates mitochondrion-to-nucleus signaling and detoxification from mitochondrial reactive oxygen species. Mol. Cell Biol. 25 (19), 8520–8530.

Suliman, S., Hemmings, S.M., Seedat, S., 2013. Brain-Derived Neurotrophic Factor (BDNF) protein levels in anxiety disorders: systematic review and meta-regression analysis. Front. Integr. Neurosci. 7, 55.

Tezcan, E., Atmaca, M., Kuloglu, M., Ustundag, B., 2003. Free radicals in patients with post-traumatic stress disorder. Eur. Arch. Psychiatr. Clin. Neurosci. 253 (2), 89–91.

Todorović, N., Tomanović, N., Gass, P., Filipović, D., 2016. Olanzapine modulation of hepatic oxidative stress and inflammation in socially isolated rats. Eur. J. Pharmaceut. Sci. 81, 94–102.

Twenge, J.M., Joiner, T.E.U.S., 2020. Census Bureau-assessed Prevalence of Anxiety and Depressive Symptoms in 2019 and during the 2020 COVID-19 Pandemic. Depress Anxiety.

Wang, T., Qin, L., Liu, B., Liu, Y., Wilson, B., Eling, T.E., et al., 2004. Role of reactive oxygen species in LPS-induced production of prostaglandin E2 in microglia. J. Neurochem. 88 (4), 939–947.

Wang, S.M., Lim, S.W., Wang, Y.H., Lin, H.Y., Lai, M.D., Ko, C.Y., et al., 2018. Astrocytic CCAAT/Enhancer-binding protein delta contributes to reactive oxygen species formation in neuroinflammation. Redox Biol. 16, 104–112.

Wang, M., Bi, Y., Zeng, S., Liu, Y., Shao, M., Liu, K., et al., 2019. Modified Xiaoyao San ameliorates depressive-like behaviors by triggering autophagosome formation to alleviate neuronal apoptosis. Biomed. Pharmacother. 111, 1057–1065.

Watanabe, S., Omran, A.A., Shao, A.S., Xue, C., Zhang, Z., Zhang, J., et al., 2022. Dihydromyricetin improves social isolation-induced cognitive impairments and astrocytic changes in mice. Sci. Rep. 12 (1), 5899.

Xing, G., Barry, E.S., Benford, B., Grunberg, N.E., Li, H., Watson, W.D., et al., 2013. Impact of repeated stress on traumatic brain injury-induced mitochondrial electron transport chain expression and behavioral responses in rats. Front. Neurol. 4, 196.

Yang, Y., Hu, Z., Du, X., Davies, H., Huo, X., Fang, M., 2017. miR-16 and fluoxetine both reverse autophagic and apoptotic change in chronic unpredictable mild stress model rats. Front. Neurosci. 11, 428.

Zheng, S., Han, F., Shi, Y., Wen, L., Han, D., 2017. Single-prolonged-stress-induced changes in autophagy-related proteins beclin-1, LC3, and p62 in the medial prefrontal cortex of rats with post-traumatic stress disorder. J. Mol. Neurosci. 62 (1), 43–54.

Zhu, G., Sun, X., Yang, Y., Du, Y., Lin, Y., Xiang, J., et al., 2019. Reduction of BDNF results in GABAergic neuroplasticity dysfunction and contributes to late-life anxiety disorder. Behav. Neurosci. 133 (2), 212–224.

Zlatković, J., Filipović, D., 2013. Chronic social isolation induces NF-κB activation and upregulation of iNOS protein expression in rat prefrontal cortex. Neurochem. Int. 63 (3), 172–179.

Zlatković, J., Todorović, N., Bošković, M., Pajović, S.B., Demajo, M., Filipović, D., 2014a. Different susceptibility of prefrontal cortex and hippocampus to oxidative stress following chronic social isolation stress. Mol. Cell. Biochem. 393 (1–2), 43–57.

Zlatković, J., Bernardi, R.E., Filipović, D., 2014b. Protective effect of Hsp70i against chronic social isolation stress in the rat hippocampus. J. Neural. Transm. 121 (1), 3–14.